Materials Characterization 131 (2017) 450–458

Contents lists available at ScienceDirect

Materials Characterization

journal homepage: www.elsevier.com/locate/matchar

Chemical composition and microstructure of zirconium oxynitride thin layers from the surface to the substrate-coating interface

G.I. Cubillos[a], M.E. Mendoza[b,c], J.E. Alfonso[d], G. Blanco[e], M. Bethencourt[f,*]

[a] Grupo de Materiales y Procesos Químicos, Departamento de Química, Universidad Nacional de Colombia, Av. Cra. 30 No 45-03, Bogotá, Colombia
[b] Metrology Materials Division, National Institute of Metrology-Inmetro, Av. Nossa Senhora das Graças 50, Xerém-Duque de Caxias, RJ 25250-020, Brazil
[c] Escuela Superior Politécnica del Litoral, ESPOL, Facultad de Ingeniería Mecánica y Ciencias de la Producción, Campus Gustavo Galindo Km 30.5 Vía Perimetral, P.O. Box 09-01-5863, Guayaquil, Ecuador
[d] Grupo de Ciencia de Materiales y Superficies, Departamento de Física, Universidad Nacional de Colombia, AA 14490 Bogotá, Colombia
[e] Department of Materials Science, Metallurgy Engineering, and Inorganic Chemistry, Faculty of Sciences, University of Cadiz, Polígono Rio San Pedro s/n, 11510 Puerto Real, Cádiz, Spain
[f] Department of Materials Science, Metallurgy Engineering, and Inorganic Chemistry, International Campus of Excellence of the Sea (CEI-MAR), University of Cadiz, Polígono Rio San Pedro s/n, 11510 Puerto Real, Cádiz, Spain

ARTICLE INFO

Keywords:
Zirconium oxinitride
Coatings
Crystal structure
Physical vapor deposition
Transmission electron microscopy
X-ray photoelectron spectroscopy

ABSTRACT

The optical, electrical and corrosion resistance properties of thin layers of zirconium oxynitride are directly related to their structure and chemical composition. In the present work a study of the chemical composition of a thin film of ZrO_xN_y from the surface to the substrate-film interface is performed, and its structure is determined. The coatings were deposited via RF magnetron sputtering, the chemical composition was analyzed by means of X-ray photoelectron spectroscopy (XPS), the microstructure was characterized by means of X-ray diffraction (XRD) patterns and transmission electron microscopy (TEM), and the morphology was analyzed via scanning electron microscopy (SEM) and atomic force microscopy (AFM). XRD and TEM analysis showed that the films exhibited two crystallographic phases: monoclinic ZrO_2 and cubic Zr_2ON_2. XPS results indicated variations in the composition of the ZrO_2 and $ZrON_2$ as a function of the depth.

1. Introduction

The importance of continuing the research on ZrO_xN_y deposited as a thin film lies in its multifunctional properties, which makes possible a wide range of combinations for generating new functional materials with integrated applications, such as: decorative, because of its variety of colors and high resistance to corrosion and mechanical properties [1,2]; electrochromic, because of its ability to modulate the degree of transparency of glass, allowing passage of only selected wavelengths; and optoelectronic, because of its ability to change its optical properties as a response to a small voltage, which allows its use in “smart windows” or X-ray mirrors [1,3,4].

ZrO_xN_y has received attention due to its excellent physical and chemical properties. Research on zirconium oxynitride (ZO_xN_y) began with J.C. Guilles in 1962, who reported three distinct phases, synthesized in a temperature from 900 °C to 2000 °C range: β(Zr_2ON_2), β($Zr_7N_4O_8$), and β′($Zr_7N_{3,2}O_{9,2}$) [5]. Subsequently, in 1992 Thomson synthesized nitride zirconia between 1400 °C and 2000 °C in nitrogen atmosphere, obtaining the β″ phase, which is similar to the β′ phase. In 1996, Martin Lerch obtained zirconium oxynitride from the solid-phase reaction ZrO_2/ZrN in nitrogen atmosphere at 1900 °C. Under these conditions, a mixture of the ZrO_2 (m) and the β″ ($Zr_7O_{9.5}N_3$) phases were synthesized. The interesting thing about this study is that the authors determined that variations in pressure between 4 and 36 bar do not produce significant changes in the phase composition, however changes in temperature at constant pressure generate changes in the crystalline phases [5,6]. The β″ phase has also been reported by Mazzoni through a process of carbonitriding of zirconia between 1350 °C and 1650 °C [7]. More recently, high-vacuum techniques for depositing thin films offer the advantage of being cost-effective processes that moderate the impact on the environment, which causes them to be widely accepted by both manufacturers and consumers. Carvalho et al. and J. Hong Huang, have used this technology to deposit zirconium oxynitride thin films by magnetron sputtering, product of their research, it is known that the properties of the ZrO_xN_y films depend on the method and coating deposit conditions, since they determine microstructural changes and chemical composition [1,2,4,8].

Unlike aliovalent doping cations, wherein the substitution is

* Corresponding author.
E-mail addresses: gcubillos@unal.edu.co (G.I. Cubillos), jealfonsoo@unal.edu.co (J.E. Alfonso), ginesa.blanco@uca.es (G. Blanco), manuel.bethencourt@uca.es (M. Bethencourt).

http://dx.doi.org/10.1016/j.matchar.2017.07.035
Received 15 February 2017; Received in revised form 17 July 2017; Accepted 17 July 2017
Available online 20 July 2017

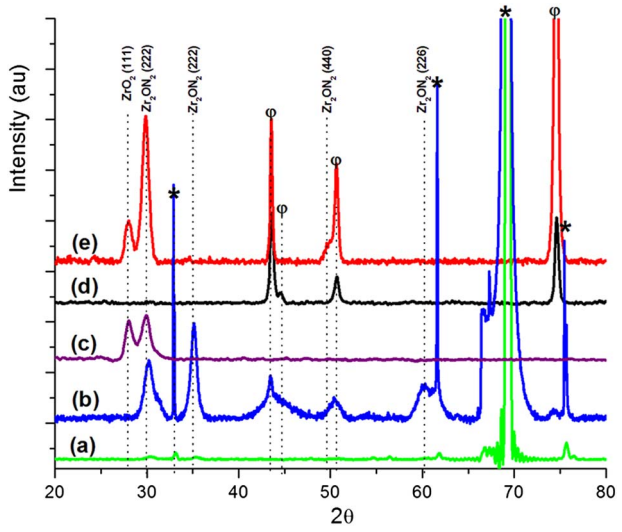

Fig. 1. XRD patterns recorded from ZrO_xN_y films deposited on AISI316L stainless steel substrates at 350 °C, 350 W. (a) Si (100), (b) coating-Si (100), (c) coating-glass, (d) AISI 316 L, (e) coating-316 L. * Phases for substrate Si (100), φ phases for substrate AISI 316 L.

completely random, replacement of oxygen with nitrogen in the crystal structure of the zirconia exhibits an array. All these phases are characterized by a fluorite-type structure organized into a super lattice. The cubic structure phase contains Zr_2ON_2 with parameters similar to those of the ZrO_2 (c) network. The β (β, β′, β″) phases exhibit a slight trigonal distortion of the cubic phase. Anion vacancies are ordered along the trigonal axis c, and for each β` phase there are different positions. The incorporation of nitrogen in a ceramic structure can improve the fracture toughness and increase the conductivity of the oxide ions [9].

It is known that the amount of nitrogen incorporated into the crystal lattice of ZrO_xN_y strongly affects its electrical properties. The maximum content of nitrogen incorporated into the matrix of zirconia that has been reported is exhibited in yttria partially stabilized zirconia 7% [4,10]. However, research related to the transport properties and their correlation with the defects in the crystal structure has not been widely reported, due to lack of methods for producing a single crystal of oxynitride.

The objective of the present investigation is to identify the crystalline phases present in the thin film of ZrO_xN_y by the techniques of DRX and TEM and to determine the changes in the chemical composition of the same from the surface to interface substrate-coating from depth profile XPS. In a previous work, we have reported the increase in the corrosion resistance of stainless steel when coated with a thin layer of ZrO_xN_y and its biocompatibility for the growth of osseous cells [11,12].

2. Experimental Method

2.1. Coating Deposition Though RF Sputtering

ZrO_xN_y films were deposited using an Alcatel HS2000, from a CERAC, Inc. Zr (99.9%) target 4 in. in diameter. The parameters used during the deposition process were based on [11]: base pressure (3.4×10^{-3} Pa); partial pressures of the gases: Ar 4.0×10^{-1} Pa, N_2 1.4×10^{-1} Pa, and O_2 2.0×10^{-1} Pa, gas flow: Ar = 20 sccm, N_2 = 2.5 sccm, and O_2 = 2.0 sccm; deposition time 30 min; target-substrate distance 5.0 cm; power supplied to the target 350 W; and substrate temperature 350 °C (623 K). The final working pressure was maintained using a valve controller for all the nitrogen flow values given above. The temperature of the substrate was measured with a type K thermocouple, and the argon, nitrogen, and oxygen flows were controlled with mass flow controllers.

2.2. Characterization of the Coatings

The crystalline structure of the films was characterized with a Panalytical X'Pert PRO X-Ray diffractometer (XRD) using Bragg-Brentano geometry with Cu-kα radiation (λ = 1.5405 Å), ranging between 10° and 90° with steps of 0.02°. The corresponding phases were identified by matching relevant data from the JCPDS (Joint Committee on Powder Diffraction Standards) cards.

TEM sample preparation was done using conventional, routine methods that involve successive steps of cutting, polishing, and ion-beam thinning with a PIPS system. The thinned specimens were measured in a Cs FEI Titan 80–300 probe, using an operating voltage of 300 kV. The instrument was equipped with an X-FEG filament and a monochromator. Conventional bright field (BF), dark field (DF), and selected area electron diffraction (SAED) images were acquired in order to analyze grain size and morphology. STEM images were acquired using a Gatan bright field-annular dark field (BF-ADF) detector with a camera length of 38 mm and convergence semi-angle α = 27.3 mrad conditions. For the chemical analysis, an EDAX analyzer was used. For TEM images and STEM-EDS, Digital Micrograph (DM) and TIA software were used, respectively, for image processing.

The surface morphology was characterized by imaging the secondary electrons using a Quanta 2000 scanning electron microscope operating at 15 kV and 10 mA, and the chemical composition of the zirconium oxynitride coatings was determined through X-ray photoelectron spectroscopy (XPS). XPS spectra were obtained with a Kratos Axis Ultra DLD instrument, equipped with a monochromatized Al Kα X-ray source (1486.6 eV), which was operated with a selected X-ray power of 150 W. XPS spectra were obtained in the constant analyzer energy (CAE) mode, with a pass energy of 20 eV for the high-resolution spectra. Depth profiles were obtained by using a Kratos Minibeam I ion source. A first set of 20 sputtering cycles consisted of Ar^+ etching at

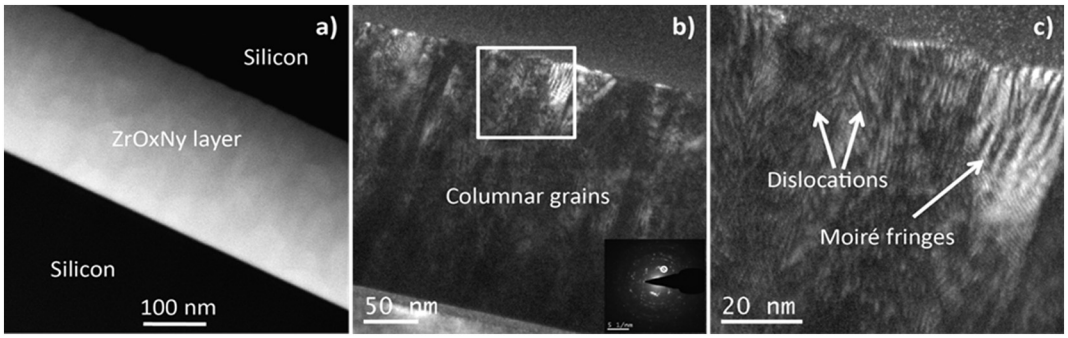

Fig. 2. a) The STEM-HAADF image shows the difference between the atomic number (Z) of the film and the substrate. b) and c) dark field images showing nano-grains diffracting in the Bragg condition. Image c) is a magnified region in the white box of image b).